Text and references accompanying Nevada Bureau of Mines and Geology Open-File Report 2022-04

Geologic Map of the Southern Diamond Mountains, Eureka and White Pine Counties, Nevada

by

Russell V Di Fiori[1,2], and Sean P. Long[1]

[1]School of Environment, Washington State University
[2]Idaho Geological Survey, University of Idaho

2022

Disclaimer: NBMG open-file reports have not been formally peer reviewed. This geologic map was funded in part by the USGS National Cooperative Geologic Mapping Program under STATEMAP award number G20AC00390, 2020.

INTRODUCTION

The Diamond Mountains are located in east-central Nevada, east and northeast of the town of Eureka (fig. 1). Early geologic mapping in the surrounding region by Nolan et al. (1962, 1971) revealed exposures of several thrust faults and folds, which have since been interpreted as part of the central Nevada thrust belt (CNTB), a system of N-striking contractional structures that branch northward off of the Sevier fold-thrust belt in southern Nevada (e.g., Taylor et al., 2000; Long, 2012, 2015; Long et al., 2014; Di Fiori et al., 2021). The southern part of the Diamond Mountains have been important for this interpretation, as they contain exposures of the Cretaceous Newark Canyon Formation (NCF), which has long been hypothesized to have been deposited during regional contractional deformation (e.g., Nolan et al., 1956; Vandervoort and Schmitt, 1990; Long et al., 2014; Long, 2015). However, there have been significant variations in interpretations of the style, timing, and magnitude of contractional deformation in the southern Diamond Mountains across multiple generations of studies (e.g., Nolan, 1962; Nolan et al., 1971; Drushke et al., 2011; Long et al., 2014). In addition, several generations of Late Cretaceous to Cenozoic normal faults have extensionally dismembered the region (Long et al., 2015), which further complicates the regional structural architecture.

In this study, our goal is to present an updated view of the structural geometry and deformational and depositional history of this complex region of central Nevada, by presenting a new 1:24,000-scale geologic map of the southern Diamond Mountains that covers an area of ~235 km^2, including the exposed extent of the NCF (fig. 1). Our field work consisted of new geologic mapping focused on two main exposures of the Newark Canyon Formation, accompanied by compilation and field-checking of key localities on the 1:31,680-scale geologic map of the Eureka 15′ quadrangle (Nolan et al., 1971) and the 1:12,000-scale map of the Eureka mining district (Nolan, 1962). We also present three retro-deformable cross sections, which illustrate the deformation geometry both above and below the modern erosion surface. This map and technical report are meant to accompany Di Fiori et al. (2020), which presents details on the stratigraphy, deposition timing, and deformational history of the NCF in the southern Diamond Mountains. This report presents detailed descriptions of members of the NCF that we defined in our mapping, as well as descriptions of Paleozoic sedimentary rock units, and explains revisions to the older structural interpretations that we have performed in our new work.

STRATIGRAPHY

A cumulative thickness of ~4.3 km of Silurian to Permian sedimentary rocks are exposed in the map area. Silurian to Devonian rocks represent the upper part of the Neoproterozoic-Devonian Cordilleran passive margin basin section (e.g., Stewart and Poole, 1974; Stewart, 1980), and are defined by thick packages of dolostone and limestone and lesser abundances of shale, sandstone, and quartzite. Mississippian rocks in the map area represent foreland basin deposits of the Antler orogeny, which were shed from the Antler highlands to the west (e.g., Speed and Sleep, 1982; Poole et al., 1992), and dominantly consist of shale, sandstone, and conglomerate. Pennsylvanian-Permian rocks consist of limestone and conglomerate and mark a period of continued shallow-marine sedimentation in eastern Nevada following the Antler orogeny (e.g., Stewart, 1980).

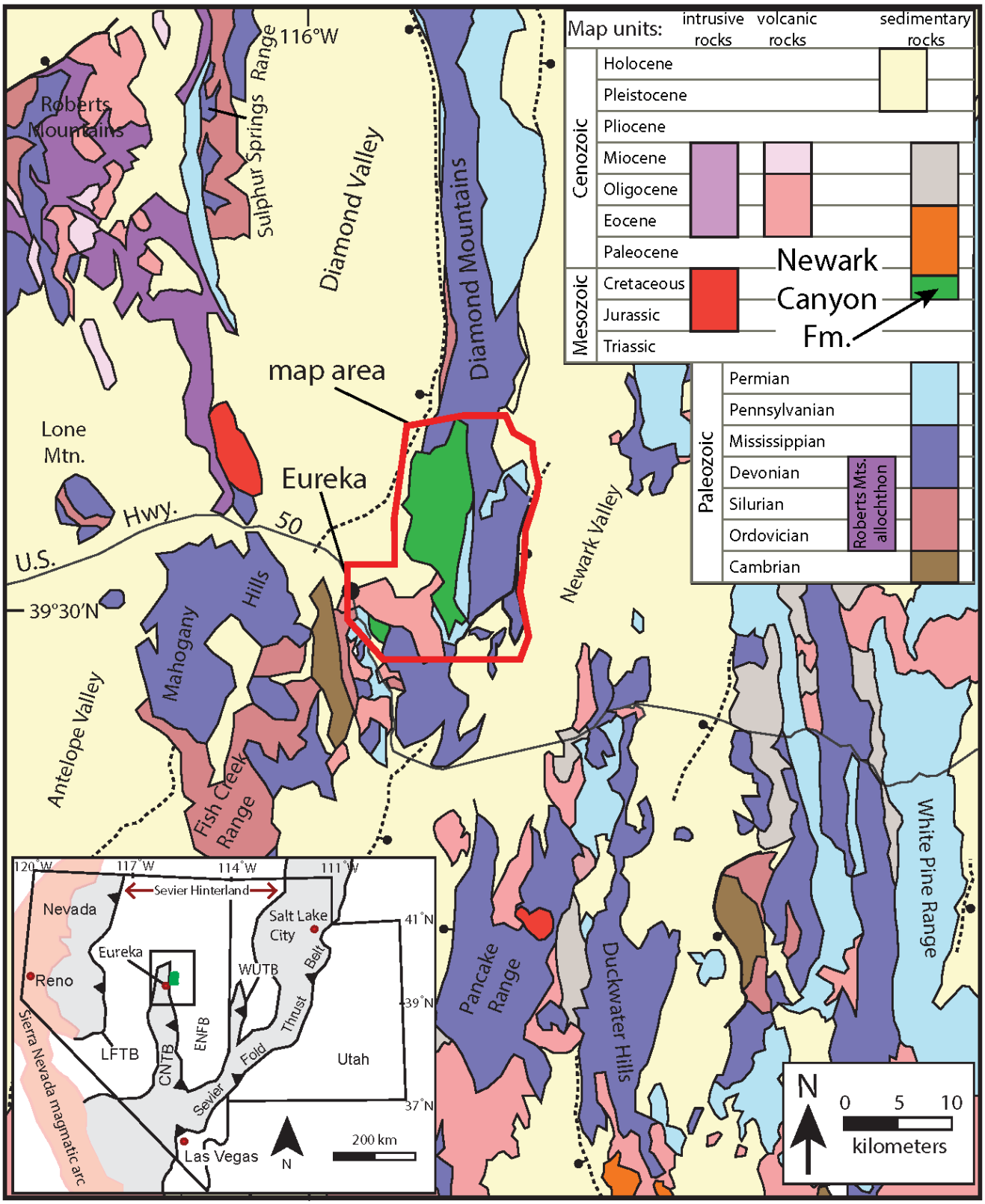

Figure 1. Geologic map of part of east-central Nevada, showing the location of the map outlined in red. Inset map in the lower left shows Cordilleran thrust systems of Nevada and Utah (shaded gray) and the Sierra Nevada magmatic arc (shaded red) (modified from Long et al., 2014). The Newark Canyon Formation exposure in the southern Diamond Mountains is shown in green. CNTB = central Nevada thrust belt; ENFB = eastern Nevada fold belt; LFTB = Luning-Fencemaker thrust belt; WUTB = Western Utah thrust belt.

Mesozoic rocks in the map include the Cretaceous Newark Canyon Formation (NCF), which consists of conglomerate, sandstone, siltstone, and fresh-water carbonate (Nolan et al., 1971; Vandervoort and Schmitt, 1990). We divided the NCF into two separate exposures; the southern of the two exposures, which contains the type-section in Newark Canyon as originally defined by MacNeil (1939), is referred to here as the 'type exposure'. North of the type exposure, along the western flank of the southern Diamond Mountains, is an extensive exposure of the NCF, which we refer to as the 'Hildebrand exposure', which is named after Hildebrand Canyon. Both exposures contain a similar internal stratigraphy, which we have divided out as five separate NCF members (Di Fiori et al., 2020): Knc_1–Knc_5. U-Pb zircon geochronology from detrital and tuffaceous horizons offers new timing constrains on deposition of the NCF within both exposures (Di Fiori et al., 2020). Maximum depositional ages, as defined by the youngest five zircon grains that overlap within error, were calculated from detrital samples collected from multiple stratigraphic levels. These data show that deposition of the basal member (Knc_1) occurred no earlier than ~114 Ma, and member Knc_3 was not deposited on earlier than ~112–106 Ma. An interval interpreted as a minimally reworked waterlain tuff was sampled from member Knc_4 in the type exposure, and the youngest population of six concordant, overlapping zircons yielded a Concordia age of 103.0 ± 0.7 Ma, which is interpreted as an actual deposition age. Finally, member Knc_5 in the type exposure was deposited no earlier than ~99 Ma. Supporting data and details on methods can be found in Di Fiori et al. (2020).

Cenozoic rocks consist mostly of Late Eocene to Oligocene felsic ignimbrites, ash-fall tuffs, and shallow intrusive rocks. The Richmond Mountain dacite (Trm) is a large, gently tilted volcanic dome (Long et al., 2014). $^{40}Ar/^{39}Ar$ geochronology from plagioclase yielded an emplacement age of 36.16 ± 0.07 Ma for this unit (Long et al., 2014). The Pancake Summit Tuff (Tps) is a porphyritic rhyolite ash-flow tuff with disseminated smoky quartz and lesser abundant sanidine phenocrysts, and is interpreted to be sourced from the Allison Creek caldera in the northeastern Monitor Hills, ~40 km west of the map (Best et al., 2009). $^{40}Ar/^{39}Ar$ geochronology from sanidine yielded and age range of 35.36 ± 0.07 to 35.40 ± 0.06 Ma for this unit (Long et al., 2014). Felsic ignimbrite, surge deposits, and ash-fall tuffs (Trt) are also common throughout the map, particularly in the northern part of the type exposure, along Newark Canyon Road. These outcrops are generally light gray to white and present in drainages. The basal surge deposits show diagnostic sedimentary depositional structures like cross-bedding and soft-sediment deformation features. Similar outcrops to the south of the map yielded K-Ar ages of 34.6 ± 1.5 Ma (Nolan et al., 1974). Rhyolite dikes (Trd), while common in the surrounding region, are only represented by a single outcrop within the map in the northern part of the Hildebrand exposure. Jasperoid, an alteration product generated when host rock has been silicified to varying degrees by hydrothermal fluids, is common in the Eureka mining district to the southwest, although only one outcrop was observed in the map. This jasperoid is an isolated, meter-scale outcrop within the western part of the Hildebrand exposure, and is spatially associated with an altered felsic(?) volcanic intrusive.

Quaternary deposits include alluvial-stream sediments and associated terraces, hillside-covering colluvium, and alluvial-fan deposits of varying ages. Older, inactive alluvial deposits (QTaf), which are topographically higher than the younger generation of alluvial-fan deposits in the map, dominate the Quaternary cover on the western flank of the Diamond Mountains, and have produced large, rounded interfluvial ridges that trend perpendicular to the range. Tertiary-Quaternary megabreccias (QTb), previously interpreted as Cretaceous (post-NCF deposition) by Nolan et al. (1971), have been reinterpreted here to be significantly younger. This interpretation is due to a volcanic rock horizon, determined to be Oligocene (Vandervoort and Schmitt, 1990), observed at the base of these immense landslide blocks, and the intercalated nature of the landslide deposits with Tertiary-Quaternary alluvial-fan deposits (QTaf). These megabreccia landslide blocks consist of angular clasts ranging in size from cm scale to tens of meters (long axis dimension of breccia clasts). Outcrops of QTb form cliffs and ledges and make up the higher topographic points within the Hildebrand exposure. Small outcrops of older gravels (QTg), which were derived from erosion of Paleozoic sedimentary rocks and include clasts of Tertiary volcanic rocks, are present in the southwestern corner of the map. Younger generations of alluvial fans (Qaf) are also exposed on the eastern flank of the Diamond Mountains and form large alluvial aprons that distribute unconsolidated sediments towards the center of the valleys. The youngest Quaternary deposits consist of hillslope colluvium (Qc) and recent alluvium (Qal) and associated alluvial terraces (Qalt) in active washes.

STRUCTURAL FRAMEWORK

Rock units and surficial deposits within the map area record multiple episodes of deformation. Folds and thrust faults, interpreted to be genetically related to regional shortening accommodated in the Late Mesozoic central Nevada thrust belt (Taylor et al., 2000; Long et al., 2014; Long, 2015; Di Fiori et al., 2020), deform rocks as old as Silurian and as young as Late Cretaceous. These contractional structures are all generally north- to northwest-striking and exhibit east-vergent geometries. These include multiple folds in Mississippian rocks within the Diamond Mountains east of the Hildebrand exposure, which were originally defined by Nolan et al. (1971). The concealed traces of two NNW-trending structures, the Sentinel Mountain syncline and the Moritz-Nager thrust, were projected northward into the southern part of the map, as they are exposed ~1–2 km to the south of our map boundary (Long et al., 2014; Nolan et al., 1974). Three new contractional structures were identified in our mapping, including (from west to east) the Strahlenberg anticline,

which is exposed within tightly folded Permian rocks, the Powerline thrust, which places Permian rocks over the NCF, and an unnamed syncline that is exposed within the middle of the NCF type exposure (Di Fiori et al., 2020). The Strahlenberg anticline and the unnamed syncline are interpreted together to represent the kink axes of an east-vergent fault-propagation fold (e.g., Suppe and Medwedeff, 1990), which generated subsidence within a synclinal basin to the east that preserves the NCF (Di Fiori et al., 2020). The Powerline thrust is interpreted to be a high-angle breakthrough thrust fault that breaches the forelimb of this fault-propagation fold (e.g., Suppe and Medwedeff, 1990; their figure 11E), and has about ~100 m of offset. In the subsurface, the Powerline thrust is interpreted to branch upward from a blind thrust at depth that was responsible for growth of the fault-propagation fold, which is interpreted to root into a flat within Mississippian units toward the west (Di Fiori et al., 2020).

The eastern side of the Diamond Mountains exhibits down-to-the-east normal faults with two scales of offset magnitude. The largest offset faults include the range-bounding fault that separates the Diamond Mountains from Newark Valley to the east. However, due to the lack of bedrock outcrop within the hanging wall, the offset magnitude is difficult to estimate. A second set of down-to-the-east normal faults, inboard of the range-bounding fault, exhibit offset magnitudes on the order of tens to hundreds of meters.

The west side of the Diamond Mountains are deformed by multiple, subparallel, down-to-the-west normal faults with varying amounts of offset. A range-bounding normal fault with an unknown amount of offset (due to the lack of bedrock outcrop in the hanging wall) defines the boundary between Diamond Valley and the Diamond Mountains. To the east of the range-bounding normal fault, a down-to-the-west normal fault deforms the steep forelimb of the Strahlenberg anticline, and exhibits ~1.2 km of offset. On the eastern flank of the Hildebrand exposure, a down-to-the-west normal fault juxtaposes the east-dipping NCF in its hanging wall against west-dipping Mississippian rocks in its footwall; this fault is estimated to have at least ~3.6 km of offset.

The southwestern corner of the map contains traces of two high-offset, N-striking normal faults, the Hoosac fault system and the Pinto Summit fault, which project southward to the mapping of Long et al. (2014). The Hoosac fault system is an anastomosing system of steeply east-dipping, down-to-the-east normal faults. The master fault of this system, which is exposed along the western edge of the map, places Permian rocks against Ordovician rocks (Long et al, 2014; 2015). The steeply-dipping, down-to-west Pinto Summit fault places Mississippian rocks against Silurian rocks (e.g., Long et al., 2014). These large-offset normal faults pre-date the l-ate Eocene sub-volcanic unconformity (Long et al., 2014, 2015). Based on cooling histories of rocks exhumed in the footwall of the Hoosac fault system, these faults have been interpreted to represent the Late Cretaceous to Paleocene (~75 60 Ma) extensional dismemberment of a regional-scale CNTB anticline, known as the Eureka culmination (Long et al., 2015).

A note on previous interpretations of the megabreccia slide blocks on the western flank of the Diamond Mountains

Megabreccia landslide deposits on the western flank of the southern Diamond Mountains are preserved as isolated outcrops within, and surrounded by, older alluvial-fan deposits (QTaf). These were originally interpreted to have been emplaced in the Cretaceous, during deposition of the NCF (Nolan et al., 1956, 1971); however, we interpret these megabreccia landslide deposits to have been emplaced during the Tertiary. Vandervoort and Schmitt (1990) described an Oligocene tuffaceous horizon at the base of some of these landslide blocks, which defines a maximum age for emplacement. Additionally, these landslide blocks are intercalated within older alluvial-fan deposits that cover much of the western flank of the Diamond Mountains. These megabreccia landslide blocks are monolithic in composition, having breccia clast compositions unique to Paleozoic source rock units. For instance, Tbcr is a megabreccia horizon defined by the breccia-clast composition sourced entirely from the Permian Carbon Ridge Formation. The structural architecture, specifically the west-dipping orientation, of the Paleozoic units within the Diamond Mountains could have generated favorable slip planes that the slide blocks exploited.

A note on previous mapping of the Mississippian Diamond Peak Formation and Chainman Shale

Distinguishing the NCF from the underlying Mississippian Diamond Peak Formation and the Permian Carbon Ridge upper conglomerate member has proven difficult in previous studies, due to similarity in lithologies and clast compositions. In the NCF type exposure, Nolan et al. (1971, 1974) mapped the basal unconformity of the NCF overlying the Permian Carbon Ridge Formation, Pennsylvanian Ely Limestone, and Mississippian Diamond Peak Formation. In our new mapping, we interpret that outcrops of the Paleozoic units immediately beneath the basal NCF unconformity to the south, southwest, and west of the type exposure of the NCF all belong to the Permian Carbon Ridge Formation upper conglomerate member, instead of the Mississippian Diamond Peak Formation. This is supported by a reconnaissance field investigation of the Permian Carbon Ridge Formation type locality in the Fish Creek Range ~15 km to the southwest of the map. This interpretation also negates the requirement for a number of complicated thrust and normal faults interpreted to be present within and west of the NCF type exposure by Nolan et al. (1971, 1974).

Within the northern part of the map, Nolan et al. (1971) mapped exposures of the Mississippian Chainman Shale structurally below the Cretaceous NCF, across a younger-over-older thrust fault with the NCF in the hanging wall. We

have re-examined these lithologies and this structural relationship, as preserved within the NCF Hildebrand exposure, and have reinterpreted the contact as a stratigraphic relationship, with the rocks previously mapped as the Chainman Shale representing a mudstone horizon at the base of the NCF. We have made this interpretation based on similar basal mudstone horizons observed in other parts of the NCF Hildebrand exposure to the west and south.

A note on previous interpretations of structures

In the Hildebrand exposure, we have mapped a previously undocumented, N- to NNE-striking, down-to-the-west normal fault, which exhibits ~1.3 km of offset and cuts the NCF. Evidence for this structure includes an abrupt across-strike change in dip magnitude and dip direction preserved in the NCF, as well as a younger (Knc_2 on the west) on older (base of Knc_1 on the east) map relationship. NCF exposures in the hanging wall of this fault dip moderately (~20–30°) to the east, while NCF outcrops in the footwall (east of the fault) are sub-vertical to overturned. We interpret that this normal fault took advantage of bedrock weaknesses generated by the construction of the east-vergent Strahlenberg anticline (see cross section A–A′, and see further explanation in Di Fiori et al., 2020).

GEOLOGIC HISTORY

The southern Diamond Mountains preserve a wide range of tectonic and depositional environments that span from the Paleozoic to the present day. Silurian and Devonian sedimentary units preserve the youngest portion of the Neoproterozoic-Devonian Cordilleran passive margin basin section, which was dominated by shallow marine carbonate deposition between the middle Cambrian and Devonian (e.g., Stewart and Poole, 1974; Stewart, 1980). During the Mississippian, Ordovician—Devonian marine basinal and slope sedimentary rocks were thrust eastward over shallow marine carbonate and clastic rocks of the continental shelf in central Nevada during the Antler orogeny, which was generated by a hypothesized arc-continent collision (e.g., Speed and Sleep, 1982; Burchfiel et al., 1992; Poole et al., 1992; Dickinson, 2004; 2006). During the Antler orogeny, the map occupied a foreland basin setting, and was the site of deposition of Mississippian clastic rocks that were shed eastward off of the Roberts Mountain allochthon to the west (e.g., Poole, 1974). After the cessation of Antler-related deformation and deposition, during the Pennsylvanian and Permian, the region again became the site of shallow marine, carbonate-dominated sedimentation (e.g., Stewart, 1980).

During the Jurassic, the development of an Andean-style subduction zone off of the western North American coast initiated construction of the North American Cordilleran orogenic belt (e.g., Allmendinger, 1992; Burchfiel et al., 1992; DeCelles, 2004; Yonkee and Weil, 2015). During the Late Jurassic to Paleogene deformation that built the Cordillera, the map lay within a broad region of Nevada referred to as the 'hinterland' of the Sevier fold-thrust belt, which was located in western Utah at this latitude (e.g., Armstrong, 1968; DeCelles, 2004). Much of the Sevier hinterland is characterized by relatively minimal contractional deformation at upper-crustal levels (e.g., Long, 2012). The region surrounding the southern Diamond Mountains lies within the Central Nevada thrust belt (CNTB), a hinterland structural province consisting of N-striking, E-vergent thrust faults and folds that branch northward off of the Sevier fold-thrust belt in southern Nevada (Taylor et al., 2000). The CNTB is estimated to have accommodated ~10 15 km of shortening (Taylor et al., 2000; Long et al., 2014). In most places, CNTB deformation can only be bracketed to be younger than Pennsylvanian-Permian, based on the youngest sedimentary rocks involved in deformation (Taylor et al., 2000). Shortening in the CNTB is interpreted to have ceased by ~85 Ma, based on crosscutting relationships with undeformed Late Cretaceous granitic intrusions (Taylor et al., 2000).

The southern Diamond Mountains contain one of the few preserved exposures of the syn-contractional NCF, which offers the opportunity to further constrain the timing of contractional deformation in the CNTB at this latitude. Our new mapping and U—Pb zircon geochronology from the NCF (Di Fiori et al., 2020) demonstrate deposition of the NCF during proximal CNTB deformation, including slip on east-vergent thrust faults and growth of east-vergent folds. Deposition of the basal NCF member was underway no earlier than ~114 Ma, a tuff in the middle part of the section was deposited at ~103 Ma, and the youngest member was deposited no earlier than ~99 Ma. Intraformational angular unconformities within the NCF, as well as abrupt along- and across-strike thickness changes, indicate that NCF deposition in the map was related to growth of an east-vergent fault-propagation fold (Di Fiori et al., 2020). CNTB deformation was therefore contemporaneous with shortening in the Sevier thrust belt at this latitude, which defines middle Cretaceous strain partitioning between frontal and interior components of the Cordillera (Di Fiori et al., 2020).

Though most of the upper-crustal extension in central Nevada did not occur until the Cenozoic, evidence for localized, Late Cretaceous-Paleocene, synorogenic extension in central Nevada has locally been documented. In the southwestern part of the map, and in proximal parts of the Fish Creek Range to the southwest, large-offset normal faults, including the Hoosac fault system and Pinto Summit fault, pre-date the late Eocene sub-volcanic unconformity (Long et al., 2014, 2015), and have been interpreted to represent the Late Cretaceous to Paleocene (~75–60 Ma) extensional collapse of a regional-scale CNTB anticline (Long et al., 2014).

During the Paleocene and Eocene, eastward migration of shortening and magmatism into Utah and Colorado during the Laramide orogeny is interpreted to represent a shallowing of the subduction angle of the Farallon plate (e.g., Smith et al., 2014). During the late Eocene and Oligocene, a northeast to southwest migration of silicic volcanism known as the Great Basin ignimbrite flare-up

swept across Nevada. This magmatic flare-up is hypothesized to be related to the post-Laramide rollback of the subducting Farallon slab (e.g., Humphreys, 1995; Smith et al., 2014). Igneous rocks generated from this event found within the map include basal surge deposits, ignimbrites, ash-fall tuffs, shallow intrusive rocks, and related volcanoclastic sedimentary rocks, all of which have yielded radiometric ages of ~36–34 Ma (Long et al., 2014).

Some spatially isolated areas of central Nevada experienced Eocene-Oligocene extension, which broadly overlapped in time with the ignimbrite flareup (e.g., Gans and Miller, 1983; Long and Walker, 2015; Lee et al., 2017). However, in the map, we see no evidence for normal faulting during emplacement of late Eocene volcanic rocks. Across Nevada, the inception of widespread extension that formed the Basin and Range Province is attributed to reorganization of the Pacific–North American plate boundary in the middle Miocene (e.g., Atwater, 1970; Dickinson, 2002, 2006). In the map, we see multiple sets of west- and east-dipping normal faults. Though most of these faults do not exhibit cross-cutting relationships with late Eocene volcanic rocks, we interpret that most are likely middle Miocene or younger in age. For example, several normal faults on the eastern flank of the Diamond Mountains are interpreted to be genetically related to the down-to-the-east range-bounding normal fault system that accommodated the subsidence of Newark Valley and uplift of the Diamond Mountains.

DESCRIPTION OF MAP UNITS

Quaternary Deposits

Qx Artificial fill (Holocene) Anthropogenically altered surfaces, including piles of broken rock, landfill material, or other significant geomorphic alterations.

Qal Active channel and transported sediments (Holocene) Poorly sorted, active alluvial sediments. Size ranges from boulders to silt. Deposited in active washes and ephemeral stream channels.

Qc Colluvium (Holocene) Veneer of poorly sorted, angular, slope-covering sediment deposited over steep slopes, mainly below ridge- and cliff-forming bedrock outcrops. Clasts range in size from silt to boulders.

Qalt Alluvial channel terrace (Holocene) Poorly-sorted, unconsolidated alluvial sediments, ranging in size from boulder to silt. These deposits are incised by active washes and ephemeral stream channels.

Alluvial-fan deposits

Qaf Active alluvial-fan deposits (Holocene) Non-lithified, silty to sandy, pebble to cobble and locally up to boulder-sized clasts deposited in active alluvial-fan systems, which onlap onto older alluvial-fan deposits. Commonly exhibit poorly developed desert pavement and armoring, as well as weak to incipient desert varnish.

Qoaf Inactive alluvial-fan deposits (Holocene to Pleistocene) Abandoned alluvial fan deposits consisting of non-lithified clasts ranging from silt to boulder size. Exhibits better-developed desert pavement and surface armoring than Qaf.

QTb Megabreccia slide blocks of Paleozoic rocks (Holocene to Oligocene) Megabreccia slide deposits on the western flank of the southern Diamond Mountains. Breccia clasts range in size from cm-scale to decameter-scale blocks. Individual slide blocks are mapped by their respective source rock unit (i.e., Tbcr was sourced from the Permian Carbon Ridge Formation). An Oligocene tuff was observed at the base of these slide blocks, indicating that they were emplaced after ~34 Ma (Vandervoort and Schmidt, 1990). Additionally, these landslide deposits are intercalated within the older alluvial fans (QTaf).

QTbe Megabreccia slide blocks of Ely Limestone Megabreccia defined by breccia clasts sourced entirely from the Pennsylvanian Ely Limestone.

QTbdp Megabreccia slide blocks of Diamond Peak Formation Megabreccia defined by breccia clasts sourced entirely from the Mississippian Diamond Peak Formation.

QTbcr Megabreccia slide blocks of Carbon Ridge Formation Megabreccia defined by breccia clasts sourced entirely from the Permian Carbon Ridge Formation.

QTaf Old inactive alluvial-fan deposits (Pleistocene to Miocene) Composed of fine sand to coarse gravel. Commonly topographically higher than the other alluvial-fan deposits, forming rounded interfluvial ridges. Exhibits advanced development of surficial armoring and desert pavement. Exposed pavement rocks exhibit well-developed desert varnish and increased abundance of vegetation coverage and density.

QTg Capping gravel (Pleistocene to Miocene) Unconsolidated gravel composed of recycled clasts derived from Paleozoic rock units. Quartzite clasts are dominant, with lesser abundances of limestone, dolostone, and rare felsic volcanic clasts. Generally preserved as elevated interfluvial ridges where deeply incised by active stream channels.

Tertiary Rocks

Tj Jasperoid breccia (Neogene) Red to brown, brecciated, and fracture-controlled hydrothermal silica, exposed in the north-center part of the map (within the Hildebrand NCF exposure). Map patterns and inherited texture indicate that the protolith is likely a shallowly emplaced dike. Forms resistant outcrops and erodes as large angular blocks.

Tps Pancake Summit Tuff (Late Eocene) Porphyritic rhyolitic ash-flow tuff, generally light gray and poorly welded. Only observed near Torre Flat; forms concentric

subdued ridges. Phenocrysts consist of ~2 mm smoky quartz and white plagioclase and significantly less abundant biotite up to ~1 mm and sanidine up to ~2 mm. Age: 35.36 ± 0.07 Ma and 35.40 ± 0.06 Ma ($^{40}Ar/^{39}Ar$ sanidine), based on two samples from Pancake Summit (Henry and John, 2013).

Trm Richmond Mountain dacite (late Eocene) Monolithic, massive to glassy and vesicular porphyritic dacite lava. Generally fine to coarse groundmass with phenocrysts mostly consisting of plagioclase and biotite with sparse quartz. Most of the outcrop extent of the Richmond Mountain dacite is in and around Richmond Mountain, where the rock erodes as large blocks, producing blocky float and talus slopes. Age is 36.16 ± 0.07 Ma ($^{40}Ar/^{39}Ar$ plagioclase; Long et al., 2014).

Trt Pyroclastic flow, ash-fall, and surge deposits White, light-pink, and gray, massive to well-bedded ash-flow tuff. Mostly poorly to moderately welded with abundant pumice up to 12 mm and lithic fragments up to 8 mm. Contains up to ~30% phenocrysts by volume, dominantly consisting of plagioclase, quartz, and lesser abundances of biotite and sanidine. Pyroclastic surge deposits make up the basal portion of outcrops and exhibit cm-scale cross-stratification. Ash-fall deposits make up the upper portion of the rock unit, and are characterized by massive to planar flow foliations and are well sorted. Exposed on hillsides and draws, makes subdued topography. Similar volcanic rocks south of the map have been dated at 34.6 ± 1.5 Ma (K—Ar biotite; Nolan et al., 1971).

Td Rhyolite dikes (Paleogene) Dikes of rhyolite or high-silica intrusive volcanic rock. Rare mm-scale plagioclase phenocrysts, but mostly aphyric. Forms discontinuous, linear, resistant, ledge-forming outcrops. Some dike outcrops are coincident with silicification alteration of the surrounding country rock.

Cretaceous Rocks

Knc Newark Canyon Formation

Knc_5 Newark Canyon Formation member 5 Brown-red to dark-gray weathering, crudely bedded and cross-stratified, poorly sorted, clast-supported pebble to cobble conglomerate. Matrix generally consists of fine to medium sand. Clast lithologies consist of white and black-speckled quartzite, red, brown, and gray chert, and rare Paleozoic carbonate. Ridge forming, where outcrops cap hill tops within the type exposure in the southern part of the map. Erodes as large blocks. U Pb geochronology from detrital zircon yielded a maximum deposition age of 98.6 ± 1.9 Ma (Di Fiori et al., 2020). Minimum thickness of ~25 m; top not exposed. Only observed in the NCF type exposure.

Knc_4 Newark Canyon Formation member 4 Yellow to brown weathering, massive to thin-bedded and locally laminated, normally graded silty biomicrite. Abundant freshwater gastropods and ostracods and fine fossil hash is present on bedding surfaces. Erodes as flakes and chips where bedding is thin, and platy where bedding is massive. Forms subdued topography with gentle slopes. A concordia age calculated from U Pb zircon geochronology from a minimally reworked, waterlain tuff within Knc_4 yielded a deposition age of 103.0 ± 0.7 Ma (Di Fiori et al, 2020). Thickness is ~90 m; only observed in the NCF type exposure.

Knc_3 Newark Canyon Formation member 3 Brown to red, poorly sorted, crudely to cross-bedded, clast-supported pebble to cobble conglomerate. Dominant clast lithology consists of gray and black chert with lesser amounts of brown, red, and green chert. Conglomerate matrix consists of medium to coarse sand. Near the top of the member, the abundance of interstitial planar and trough cross-stratified to massive sandstone increases. U—Pb geochronology from detrital zircon yielded maximum deposition ages of 112.9 ±1.0 Ma (type exposure) and 106.0 ± 1.5 Ma (Hildebrand exposure) (Di Fiori et al., 2020). Thickness is ~105 to ~295 m.

Knc_2 Newark Canyon Formation member 2 Red, yellow, to gray-mottled, cm-scale silty micrite, siltstone, and micrite. Interbedded with brown, tan, gray, and red, moderately sorted, massive to horizontally bedded sandstone, which becomes more dominant towards the top of the member. Sandstone is dominated by chert and quartzite clasts. Liesegang iron-oxide banding is pervasive and common. Thickness is ~95 to ~170 m.

Knc_1 Newark Canyon Formation member 1 Red to gray weathering, clast-supported pebble to cobble conglomerate lenses within pink, yellow, to gray massive to laminated micrite and silty-micrite. Micrite and siltstone are the dominant lithologies by volume but are poorly exposed. Conglomerate clast lithologies consist largely of Paleozoic carbonate pebbles and cobbles with fusulinid and crinoid fossils. Lithofacies in this member change abruptly over short lateral distances. Lesser abundant clast lithologies include red, brown, gray, and green chert. In the Hildebrand exposure, a blue-gray, dark-gray, to purple-gray basal silty mudstone (~2 m minimum thickness) is present within incised ravines. Locally displays a pronounced angular discordance with the underlying Pcru. U—Pb geochronology from detrital zircon yielded a maximum deposition age of 113.7 ± 2.3 Ma (Di Fiori et al., 2020). Between ~100 and ~500 m thick.

Paleozoic Rocks

Pcru Carbon Ridge Formation, upper conglomerate (Lower Permian) Gray, tan, to red weathering, chert-clast supported pebble conglomerate with calcareous cement matrix. Clast lithology dominated by sub-rounded, gray and

green chert. Matrix consists of fine to medium sand. Conglomerate is interbedded with cm-scale gray fusulinid-rich limestone. Exhibits an interfingering contact with unit Pcrl below. At least ~445 m thick.

Pcrl Carbon Ridge Formation, lower limestone (Lower Permian) Gray to brown weathering, thin to medium bedded, silty micrite to silty limestone. Interbedded fusulinid-rich limestone beds are also common, sometimes exhibiting fossil hash. Thin-bedded, interstitial, cross-stratified carbonaceous red siltstone, fine-grained sandstone, and chert-pebble conglomerate are also present but rare. Rare decameter-scale concretions weather out of the fine-grained horizons. Forms gentle hillslopes and erodes as platy and blocky float. Lower contact with unit IPe is a sharp, erosional unconformity. Maximum thickness is ~610 m.

IPe Ely Limestone (Lower Pennsylvanian) Massive to thick-bedded, light-gray to bluish-gray limestone with diagnostic nodular brown, tan, and red-brown weathering chert. Interbedded sandstone and rare conglomerate at base. Ledge and ridge-forming; erodes to form blocky float. Thickness is ~510 m.

Mdp Diamond Peak Formation (Upper Mississippian) Brown to red weathering, chert clast supported, sub-rounded pebble conglomerate. Conglomerate clast lithology is defined by gray, white, green, red, and brown chert with calcareous sandstone matrix. Conglomerate is interbedded with medium to coarse, red-brown to gray sandstone. Exhibits rare wood and horsetail (Calamites) casts in fine-medium sandstone horizons. Abrupt lateral variations in lithology (i.e., limestone to conglomerate within ~20 m). Ridge- and ledge-forming; erodes as large blocks. Up to 880 m thick, though thickness could be exaggerated by intraformational folding and faulting.

Mc Chainman Shale (Upper Mississippian) Black to green-tan weathering, thin-bedded to thinly laminated shale with lesser interstitial red and brown, fine- to medium-grained sandstone and clast-supported, chert pebble conglomerate. Pencil cleavage is common, as the majority of the rock unit records m- and km-scale folding. Outcrop exposure is generally very poor, forming subdued topography while eroding as fissile and chippy float. The best outcrop exposure is found in road cuts along Newark Canyon Road. Estimated thickness is ~650 m, but this is likely exaggerated due to intraformational deformation.

Mj Joana Limestone (Lower Mississippian) Tan, buff, to brown weathering, medium and well-bedded porcelaneous limestone. Limestone is dark gray to blue-gray on fresh surfaces. Diagnostic sandy crinoid-dominant fossiliferous limestone beds. Locally conglomeratic, nodular cherty limestone, black platy shale, and thin sandstone beds. Thin red-brown siliceous stringers are common throughout outcrops. ~60 m thick. Description from Nolan et al. (1956; 1971).

Dp Pilot Shale (Lower Mississippian to Upper Devonian) Yellow, yellow-green, and buff weathering laminated calcareous siltstone and shale. Freshly broken surfaces are black to dark-green. Interstitial thin-bedded silty-limestone. Erodes in small plates forming subdued topography; does not outcrop well. ~100 m thick. Description from Nolan et al. (1956; 1971).

Ddg Devil's Gate Limestone (Upper to Middle Devonian)

Ddghc Hayes Canyon member Blue-gray, medium- to thick-bedded with local horizons of massive limestone. Tan to buff, laminated, undulatory siltstone partings are common throughout the outcrop and form platy float. Limestone is fossil-rich, and includes crinoids, stromatoporoids, and gastropods. Dark chert horizons near the top and oolitic limestone beds at the base of the member. ~275 thick. Description from Nolan et al. (1956; 1971).

Ddgm Meister member Dark-gray to blue-gray, thin-bedded dolomitic limestone with interbedded tan to pink weathering, thin- to medium bedded, laminated dolostone. Less common interstitial tan and pink-weathering siltstone. Common occurrence of Cladopora and Stromatopora corals. Erodes into platy float, forming ledges and steep hillsides. ~150 m thick. Description from Nolan et al. (1956; 1971).

Dbs Bay State Dolomite (Lower Devonian) Gray, massive to medium-bedded dolostone. Lesser abundances of laminated dark-brown and light gray dolostone are common. Characteristic "spaghetti" Cladopora cylindrical coral. Crops out very well and forms cliffs. Erodes as blocky slopes. ~220 m thick. Description from Nolan et al. (1956; 1971).

Dw Woodpecker Limestone (Lower Devonian) Dark-gray thin-bedded, sandy- to argillaceous limestone with interbedded pink to tan siltstone. Siltstone partings locally weather red to pink. Erodes as diagnostic platy and flaggy float of pink siltstone and dark-gray limestone, respectively. Forms subdued ledges and steep hillslopes; outcrops poorly, commonly found in strike-valleys. ~150 m thick. Description from Nolan et al., (1956; 1971).

Dsm Sentinel Mountain Dolomite (Lower Devonian) Light-gray, dark-gray, to brown well-bedded dolostone. Alternating bedding color is diagnostic. Light-gray dolostone is massive to thick-bedded. Brown dolostone horizons are thick- to medium-bedded. Both light-gray and brown dolostone exhibit local, faint, laminated horizons and exhibit cm-scale, striped, mottled texture. Forms resistant ridges and brown cliffs, and erodes into blocky float. ~180 m thick. Description from Nolan et al. (1956; 1971).

Dox Oxyoke Canyon Sandstone (Lower Devonian) Light-gray, light-brown, to olive-gray cross-stratified dolomitic sandstone within a dolomitic cement. Massive interbedded, gray dolomite is common. Sand is dominantly quartz and generally coarse-grained, moderately sorted, and subangular. Crinoid stem casts in the lower beds. Weathers tan, buff, to brown, and erodes as blocks. Forms resistant

brown ledges and cliffs. Description from Nolan et al. (1956; 1971).

Dbp Beacon Peak Dolomite (Lower Devonian) Light-gray, olive, to creamy-gray, thin- to medium-bedded porcelaneous dolostone. Bedding is well-developed, with interstitial, massive to thick-bedded white dolostone. Dolostone is also locally laminated. Interbedded, thin-bedded brown sandstone beds near the upper contact. Fracture-controlled siliceous stringers are common and pervasive. Commonly breaks along conchoidal fractures. Erodes as large blocks, and forms gray bluffs and ledges. ~250 m thick. Description from Nolan et al. (1956; 1971).

Dbpq Beacon Peak Dolomite, basal quartzite (Lower Devonian) Gray to white, moderately sorted, massive quartzite, with local dolomitic composition. Quartz grains are medium- to coarse-grained, well-sorted and subangular. Weathers light- to medium-gray, forming blocky float. Forms resistant ledges and outcrops well. Brecciation and pervasive fracturing are very common. ~30 m thick. Description from Nolan et al. (1956; 1971).

Slm Lone Mountain Dolomite (Silurian) Gray to light-gray, massive- to thick-bedded dolomite. Dolomite is coarse and exhibits a saccharoidal texture. Crinoid fossil hash is common at the base. Weathers in large blocks from ledges and cliffs. Fracture-controlled, red-brown silicification and brecciation is common. Forms prominent and rugged exposures. ~400 m minimum thickness. Description from Nolan et al. (1956; 1971).

Ohc Hanson Creek Formation (Upper Ordovician) Black to dark-gray typically fine-grained dolostone interbedded with tan to green thin-bedded micrite. The micrite is bioclastic, generally exhibiting crinoid hash, and is more abundant at the top of the section.

ACKNOWLEDGMENTS

Research supported by the U.S. Geological Survey, National Cooperative Geologic Mapping Program, under USGS agreement number G20AC00390. The views and conclusions contained in this document are those of the authors and should not be interpreted as necessarily representing the official policies, either expressed or implied, of the U.S. Government.

Field mapping and geochronology analyses supported by funding from the National Science Foundation, grant EAR-1524765 awarded to Long. Di Fiori would also like to thank Kevin Rafferty for assistance in the field.

REFERENCES

Atwater, T., 1970, Implications of plate tectonics for the Cenozoic evolution of North America: Geological Society of America Bulletin, v. 81, p. 3513–3536.

Allmendinger, R.W., 1992, Fold and thrust tectonics of the western United States exclusive of the accreted terranes, *in* Burchfiel, B.C., et al., editors., The Cordilleran orogen–conterminous U.S.: Boulder, Colorado, Geological Society of America, Geology of North America, v. G-3, p. 583–607.

Armstrong, R.L., 1968, Sevier orogenic belt in Nevada and Utah. Geological Society of America Bulletin. 79, 429–458.

Best, M.G., Barr, D.L., Christiansen, E.H., Gromme, S., Deino, A.L., and Tingey, D.G., 2009, The Great Basin Altiplano during the middle Cenozoic ignimbrite flareup—insights from volcanic rocks–International Geology Review, v. 51, p. 589–633.

Burchfiel, B.C., Cowan, D.S., and Davis, G.A., 1992, Tectonic overview of the Cordilleran orogen in the western United States, *in* Burchfiel, B.C., Lipman, P.W., and Zoback, M.L., editors., The Cordilleran orogen—conterminous U.S.: Boulder, Colorado, Geological Society of America, The Geology of North America, v. G-3, p. 407–480.

DeCelles, P.G., 2004, Late Jurassic to Eocene evolution of the Cordilleran thrust belt and foreland basin system, western U.S.A.: American Journal of Science, v. 304, p. 105–168.

Dickinson, W.R., 2002, The Basin and Range Province as a composite extensional domain: International Geology Review, v. 44, p. 1–38.

Dickinson, W.R., 2004, Evolution of the North American Cordillera: Annual Review of Earth and Planetary Sciences, v. 32, p. 13–44.

Dickinson, W.R., 2006, Geotectonic evolution of the Great Basin: Geosphere, v. 2, p. 353–368.

Di Fiori, R.V., Long, S.P., Fetrow, A.C., Snell, K.E., Bonde, J.W., and Vervoort, J., 2020, Syncontractional deposition of the Cretaceous Newark Canyon Formation, Diamond Mountains, Nevada—implications for strain partitioning within the U.S. Cordillera: Geosphere, v. 16.

Di Fiori, R.V., Long, S.P., Fetrow, A.C., Snell, K.E., Bonde, J.W., and Vervoort, J.D., 2021, The role of shortening in the Sevier hinterland within the U.S. Cordilleran retroarc thrust system—insights from the Cretaceous Newark Canyon Formation in central Nevada: Tectonics, 40, e2020TC006331.

Druschke, P., Hanson, A.D., Wells, M.L., Gehrels, G.E., Stockli, D., 2011, Paleogeographic isolation of the Cretaceous to Eocene Sevier hinterland, east-central Nevada—insights from U–Pb and (U–Th)/He detrital zircon ages of hinterland strata: Geological Society of America Bulletin 123, p. 1141–1160.

Gans, P.B., and Miller, E.L., 1983, Style of mid-Tertiary extension in east-central Nevada: Utah Geological and Mineral Survey Special Studies 59, p. 107–160.

Henry, C.D., and John, D.A., 2013, Magmatism, ash-flow tuffs, and calderas of the ignimbrite flareup in the western Nevada volcanic field, Great Basin, USA: Geosphere, v. 9, p. 951–1008.

Humphreys, E.D., 1995, Post-Laramide removal of the Farallon slab, western United States: Geology, v. 23, p. 987–990.

Lee, J., Blackburn, T., and Johnston, S., 2017, Timing of mid-crustal ductile extension in the northern Snake Range metamorphic core complex, Nevada: Evidence from U/Pb zircon ages: Geosphere, v. 13(2), p. 439–459.

Long, S.P., 2012, Magnitudes and spatial patterns of erosional exhumation in the Sevier hinterland, eastern Nevada and western Utah, USA—insights from a Paleogene paleogeologic map: Geosphere, v. 8, p. 881–901.

Long, S.P., 2015, An upper-crustal fold province in the hinterland of the Sevier orogenic belt, eastern Nevada, U.S.A.—a Cordilleran valley and ridge in the Basin and Range: Geosphere, v. 11, p. 404–424.

Long, S.P., Thomson, S.N., Reiners, P.W., and Di Fiori, R.V., 2015, Synorogenic extension localized by upper-crustal

thickening: an example from the Late Cretaceous Nevadaplano: Geology, v. 43, p. 351–354.
Long, S.P., and Walker, J.P., 2015, Geometry and kinematics of the Grant Range brittle detachment system, eastern Nevada, U.S.A.–an end-member style of upper-crustal extension: Tectonics, v. 34, p. 1837–1862.
Long, S.P., Henry, C.D., Muntean, J.L., Edmondo, G.P., and Cassel, E.J., 2014, Early Cretaceous construction of a structural culmination, Eureka, Nevada, U.S.A. implications for out-of-sequence deformation in the Sevier hinterland: Geosphere, v. 10, p. 564–584.
MacNeil, F.S., 1939, Fresh-water invertebrates and land plants of Cretaceous age from Eureka, Nevada: Journal of Paleontology, v. 13, p. 355–360.
Nolan, T.B., Merriam, C.W., and Williams, J.S., 1956, The stratigraphic section in the vicinity of Eureka, Nevada: U.S. Geological Survey Professional Paper 276, 77 p.
Nolan, T.B., 1962, The Eureka mining district, Nevada: U.S. Geological Survey Professional Paper 406, 78 p.
Nolan, T.B., Merriam, C.W., and Brew, D.A., 1971, Geologic Map of the Eureka quadrangle, Eureka and White Pine counties, Nevada: U.S. Geological Survey Miscellaneous Investigations Series Map I-612, 2 plates, scale 1: 31,680, 8 p.
Nolan, T.B., Merriam, C.W., and Blake, M.C., Jr., 1974, Geologic map of the Pinto Summit quadrangle, Eureka and White Pine counties, Nevada: U.S. Geological Survey Miscellaneous Investigations Series Map I-793, 2 plates, scale 1: 31,680, 14 p.
Poole, F.G., 1974, Flysch deposits of Antler foreland basin, western United States, *in* Dickinson, W.R., editor., Tectonics and sedimentation: Society of Economic Paleontologists and Mineralogists Special Publication 22, p. 58–82.
Poole, F.G., Stewart, J.H., Palmer, A.R. Sandberg, C.A., Madrid, R.J., Ross, R.J., Jr., Hintze, L.F., Miller, M.M., and Wricke, C.T., 1992, Latest Precambrian to latest Devonian time; development of a continental margin, *in* Burchfiel, B.C., Lipman, P.W., and Zoback, M.L., editors., The Cordilleran orogen—conterminous U.S.: Boulder, Colorado, Geological Society of America, The Geology of North America, v. G-3, p. 9–56.
Smith, M.E., Carroll, A.R., Jicha, B.J., Cassel, E.J., and Scott, J.J., 2014, Paleogeographic record of Eocene Farallon slab rollback beneath western North America: Geology, v. 42.
Speed, R.C., and Sleep, N., 1982, Antler orogeny and foreland basin—a model: Geological Society of America Bulletin, v. 93, p. 815–828.
Stewart, J.H., 1980, Geology of Nevada—a discussion to accompany the geologic map of Nevada: Nevada Bureau of Mines and Geology Special Publication 4, 136 p.
Stewart, J.H., and Poole, F.G., 1974, Lower Paleozoic and uppermost Precambrian Cordilleran miogeocline, Great Basin, western United States, *in* Dickinson, W.R., editor, Tectonics and sedimentation: SEPM (Society of Economic Paleontologists and Mineralogists) Special Publication 22, p. 28–57.
Suppe, J., and Medwedeff, D.A., 1990, Geometry and kinematics of fault-propagation folding: Eclogae Geologicae Helvetiae, v. 83, p. 409–454.
Taylor, W.J., Bartley, J.M., Martin, M.W., Geissman, J.W., Walker, J.D., Armstrong, P.A., and Fryxell, J.E., 2000, Relations between hinterland and foreland shortening: Sevier orogeny, central North American Cordillera: Tectonics, v. 19, p. 1124–1143.
Vandervoort, D. S., and Schmitt, J. G., 1990, Cretaceous to early Tertiary paleogeography in the hinterland of the Sevier thrust belt, east-central Nevada: Geology, v. 18, p. 567–570.
Yonkee, W.A., and Weil, A.B., 2015, Tectonic evolution of the Sevier and Laramide belts within the North American Cordillera orogenic system: Earth-Science Reviews, v. 150, p. 531–593.

Suggested Citation

Di Fiori, R.V., and Long, S.P., 2022, Geologic map of the southern Diamond Mountains, Eureka and White Pine counties, Nevada: Nevada Bureau of Mines and Geology Open-File Report 2022-04, scale 1:24,000, 10 p.